Author Manuscript

Author Manuscript

Author Manuscript

Author Manuscript

HHS Public Access

Author manuscript

Genesis. Author manuscript; available in PMC 2016 April 13.

Published in final edited form as:

Genesis. 2015 March ; 53(0): 270–277. doi:10.1002/dvg.22850.

prdm1a functions upstream of *itga5* in zebrafish craniofacial development

Kristi LaMonica[1,2], **Hai-lei Ding**[1,3], and **Kristin Bruk Artinger**[1,*]

[1]Department of Craniofacial Biology, School of Dental Medicine, University of Colorado Anschutz Medical Campus, Aurora, CO 80045, USA

Abstract

Cranial neural crest cells are specified and migrate into the pharyngeal arches where they subsequently interact with the surrounding environment. Signaling and transcription factors, such as *prdm1a* regulate this interaction, but it remains unclear which specific factors are required for posterior pharyngeal arch development. Previous analysis suggests that *prdm1a* is required for posterior ceratobranchial cartilages in zebrafish and microarray analysis between wildtype and *prdm1a* mutants at 25 hours post fertilization demonstrated that integrin α5 (*itga5)* is differentially expressed in *prdm1a* mutants. Here, we further investigate the interaction between *prdm1a* and *itga5* in zebrafish craniofacial development. In situ hybridization for *itga5* demonstrates that expression of *itga5* is decreased in *prdm1a* mutants between 18- 31 hpf and *itga5* expression overlaps with *prdm1a* in the posterior arches, suggesting a temporal window for interaction. Double mutants for *prdm1a;itga5* have an additive viscerocranium phenotype more similar to *prdm1a* mutants, suggesting that *prdm1a* acts upstream of *itga5.* Consistent with this, loss of posterior pharyngeal arch expression of *dlx2a*, ceratobranchial cartilage 2-5, and cell proliferation in *prdm1a* mutants can be rescued with *itga5* mRNA injection. Taken together, these data suggest that *prdm1a* acts upstream of *itga5* and are both necessary for posterior pharyngeal arch development in zebrafish.

Keywords

ceratobranchials; pharyngeal arches; and neural crest

Introduction

Neural crest cells (NCCs) are a transient cell population that arises at the junction between the neural and non-neural ectoderm. NCCs delaminate from the dorsal neural tube and migrate to distant sites where they differentiate into a variety of tissues. NCCs can be subdivided into 2 groups, cranial and trunk: Trunk NCCs gives rise to enteric neurons, pigment cells, and sensory nerves and glia, while cranial neural crest cells (cNCCs) give rise to neurons and glia of the cranial ganglia, connective tissue, in addition to cartilage and bone

*To whom all correspondence should be addressed: T: 303-724-4562 F: 303-724-4580 Kristin.Artinger@ucdenver.edu.

[2]Current Address: Department of Biology, Russell Sage College, Troy, NY 12180 USA

[3]Current Address: Laboratory of Anesthesiology, Xuzhou Medical College, Jiangsu 221004, China

Author Manuscript Author Manuscript Author Manuscript Author Manuscript

of the craniofacial skeleton (Le Douarin 1982; Schilling and Kimmel 1994; Graham 2003; Chai and Maxson 2006).

cNCCs begin delaminating and migrating at 12 hours post fertilization (hpf) in the zebrafish (*Danio rerio*); migrating in 3 distinct streams to ultimately populate the pharyngeal arches (PAs). The PAs are finger like projections in which cNCCs migrate into to form a mesenchyme with the mesoderm, surrounded by an outer layer of ectoderm and inner layer of endoderm (Graham 2003). These four tissue types interact through a wide variety of signaling pathways such as the FGF, Retinoic Acid, Wnt, and Endothelin families to direct differentiation of the PAs into the craniofacial skeleton (Clouthier et al. 2000; Bachler and Neubuser 2001; Clouthier and Schilling 2004; Eberhart et al. 2006; Kopinke et al. 2006; Nechiporuk et al. 2007; Blentic et al. 2008; Sperber and Dawid 2008). Posterior PA derivatives contribute to the gill slits in zebrafish and laryngeal cartilages in mammals.

The zinc finger containing transcription factor *prdm1a* plays an important role in posterior pharyngeal arch development in zebrafish and mice (Hernandez-Lagunas et al. 2005; Wilm and Solnica-Krezel 2005; Birkholz et al. 2009). *prdm1a* mutants in zebrafish have a loss of posterior ceratobranchial cartilages (CBs) 2-5 due to a reduction in cell proliferation (Birkholz et al. 2009). To further understand signaling downstream of *prdm1a*, we performed microarray analysis of *prdm1a* mutant embryos at 25 hpf compared to wildtype or heterozygous embryos. *integrin α5 (itga5)* expression is reduced in the pharyngeal arches of *prdm1a* mutants (Olesnicky et al. 2010). In addition, bioinformatics analysis suggests that the *itga5* promoter contains a canonical *prdm1a* binding site (GAAAG), suggestive of a direct interaction.

Integrins are transmembrane receptors that bind to extracellular matrix as alpha and beta heterodimers to promote cell adhesion and migration. *itga5* is expressed and functions in multiple tissue layers including mesoderm in both mice and zebrafish, and endoderm in zebrafish. Null *itga5* mice are embryonic lethal due to mesodermal defects that result in a lack of posterior somites and paraxial mesoderm formation resulting in the inability of the embryo to turn (Yang et al. 1993). Zebrafish *itga5* has been shown to function in the endoderm to pattern the PA2 neural crest during formation of the lateral hyoid cartilage (Crump et al. 2004), as well as interacting with Fgf signaling in the posterior cranial placodes (Bhat and Riley 2011), and has been shown to be required for somite boundaries and maintenance (Koshida et al. 2005; Julich et al. 2009). Here we demonstrate by double mutant and RNA rescue analysis that *itga5* functions downstream of *prdm1a*.

Results

To determine the expression of *itga5* specifically in the posterior pharyngeal arches of wildtype and *prdm1a* mutant embryos, we performed in situ hybridization (ISH) between 11- 31 hpf. Consistent with published data (Crump et al. 2004; Olesnicky et al. 2010), we observe expression of *itga5* at 11-20 hpf at the neural plate border between the neural plate and the non-neural ectoderm that includes cNCCs and ectodermal placodal cells (Figure 1A–C). As development progresses, *itga5* is strongly expressed in the pharyngeal arch region (Figure 1D, E). In *prdm1a* mutant embryos *itga5* expression is decreased at 11, 13,

Author Manuscript Author Manuscript Author Manuscript Author Manuscript

20 and 31 hpf (Figure 1A′, B′, C′, D′, E′) compared to wildtype embryos (Figure 1A, B, C, D, E). These data show that *itga5* is expressed in the PAs, is reduced in *prdm1a* mutant embryos, and that its spatiotemporal expression pattern is similar to *prdm1a* in the posterior PAs (Birkholz et al. 2009). Interestingly, *prdm1a* expression is also decreased in *itga5* mutant embryos at 24 hpf and 31 hpf (Supplemental Figure 1). To determine if both *prdm1a* and *itga5* are expressed in the same tissue we utilized the *Tg(prdm1a*:GFP) transgenic fish line and performed double fluorescent ISH for DIG labeled *itga5* and Fluorescein labeled GFP for *prdm1a* at 31 hpf. We observe expression in of *itga5* and *prdm1a* in the same region of the posterior PAs (arrow in Figure 1F), but not in the fin bud and hatching gland where *prdm1a* is also expressed at this stage (Figure 1F, F′, F″). This localization suggests that *prdm1a* and *itga5* expression overlaps in the posterior PAs and may function together to regulate posterior PA development.

To determine if there is a genetic interaction between *itga5* and *prdm1a* we performed a double mutant analysis. Heterozygotous *itga5*$^{+/-}$ and *prdm1a*$^{+/-}$ zebrafish were crossed to generate *itga5*$^{-/-}$*; prdm1a*$^{-/-}$ embryos and assayed for the presence of posterior CBs with alcian blue. Based on the expected ratios, only 1 out of 16 embryos will be double mutant; we identified *itga5*$^{-/-}$*; prdm1a*$^{-/-}$ double mutants, confirmed by genotyping followed by alcian blue processing at 5 days post fertilization (dpf). Single *prdmla* mutant embryos display an overall hypoplasia of the viscerocranium in addition to a loss of posterior CB cartilages 3-5, with only CB1 and sometimes CB2 present, consistent with our previous data (50% of time CB2 is present; Figure 2B, B′). As described previously, *itga5* mutants display a viserocranium cartilage phenotype that is highly variable (Crump et al. 2004). In some embryos, we observe a hypoplastic foramen of the hyosymplectic derived from the hyoid arch (PA2) (50% of the time we observe a reduced or absent hypoplastic hyosymplectic; as seen in double mutants Figure 2D′, arrow). In addition, the posterior CBs 4-5 are absent in *itga5* mutant embryos. In a subset of i*tga5* mutants we observe a fusion between CBs 1 and 2 and a subsequent loss of the remaining CBs often occurring on one side (12.5% have fused CB1 and 2; Figure 2C, C′). However, some genotyped *itga5a* mutant embryos display normal morphology of the hyoid arch (50% normal morphology; Figure 2C, C′). Analysis of double *itga5*$^{-/-}$*; prdm1a*$^{-/-}$ mutant embryos is suggestive of an additive effect on the posterior PA and hyosympletic cartilage development. Double *itga5*$^{-/-}$*; prdm1a*$^{-/-}$ mutant embryos lack CBs 2-5, similar to that of *prdm1a* mutants alone (Figure 2D, D′). In addition, there is an increase in the incidence of the reduction in size or absence of the foreman of the hyosymplectic cartilage (80% affected; with 40% reduced, 40% absent and 20% normal; Figure 2D, D′). These data show that loss of both *prdm1a* and *itga5* leads to an additive phenotype that is more severe than loss of either gene alone, suggestive of a genetic interaction.

To determine if there is an epistatic relationship between *itga5* and *prdm1a*, we injected *itga5* mRNA into *prdm1a* morphants (or mutants) to determine whether *itga5* mRNA injected into *prdm1a* morphants is sufficient to rescue the posterior CB phenotype. *prdm1a* morphants display phenotypes similar to *prdm1a* mutants, with loss of CB3-5 as well as a variable inversion of the ceratohyal cartilage at 5–6 dpf and a reduction of posterior arch expression of the postmigratory cNCC and PA marker *dlx2a* at 36 hpf, as we have shown

Author Manuscript Author Manuscript Author Manuscript Author Manuscript

previously (Figure 3B, F)(Birkholz et al. 2009). At doses of *itga5a* mRNA injected (between 50–112pg) into wildtype embryos, there were no obvious defects in viserocranium cartilage formation at 5 dpf or *dlx2a* expression at 36 hpf (Figure 3C, G). However, when 90 pg of *itga5* mRNA was injected into *prdm1a* morphants and stained with alcian blue at 5 dpf, 79% of *prdm1a* morphant embryos injected with *itga5* mRNA displayed 3 or more CBs at 6 dpf (Figure 3D, I), compared to *prdm1a* morphants (Figure 3B, I). We observed similar rescue with both 50 and 112 pg of *itga5* mRNA injected into morphants as compared to *itga5* mRNA injected embryos (data not shown). In addition, whereas most *prdm1a* morphants display only anterior PA expression of *dlx2a*, injection of *itga5a* mRNA rescues post-migratory NC expression of posterior *dlx2a* (Figure 3H, J), compared to uninjected controls (Figure 3F, J) and *prdm1a* morphants (Figure 3B, J) and mutants (data not shown). Quantification of the number of CBs and *dlx2a* expression is shown in Figure 3I, J.

In *prdm1a* mutants, there is a reduction of proliferation in the posterior arch region, and we hypothesize that a potential mechanism for the rescue of the *prdm1a* mutant phenotype with *itga5* mRNA is through a recovery of cell proliferation. We stained *prdm1a* mutants, *itga5* mRNA injected embryos and *prdm1a* mutants injected with *itga5* mRNA and quantified the amount of proliferation as labeled by phosphohistone H3 immunofluorescence in the posterior arch region. We determined that proliferation was significantly increased in *prdm1a* mutants injected with *itga5* mRNA ($P<0.05$) (Figure 4) compared to *prdm1a* mutants alone (Figure 4).

Our data demonstrate that *itga5* is downstream of *prdm1a* and that injection of *itga5* mRNA is sufficient to rescue the *prdm1a* mutant phenotype through an increase in cell proliferation. Canonically, *itga5* acts as part of a heterodimer with *itgb1* as a transmembrane receptor where *itga5* interacts with fibronectin exclusively extracellularly (Harburger and Calderwood 2009). Intracellularly, the cytoplasmic tail of *itgb1* is known to interact with α-actinin, vinculin, and paxillin for cell migration (Harburger and Calderwood 2009). Focal adhesion kinase (FAK) is also downstream of the integrin heterodimer and FAK plays known roles in both migration and proliferation through MAP kinase signaling via ERK (Fromigue et al. 2012). *itgb1* expression via mRNA in situ hybridization is relatively unchanged in *prdm1a* mutants, which is not unexpected since *itgb1* is known bind with other alpha subunits and not exclusively with *itga5* (data not shown). The expression pattern of *itgb1* is also more diffuse throughout the embryo, possibly reflecting localization of its other binding partners. Specifically, *itga5* has been shown to play a role in inducing proliferation and differentiation in bone and in dental pulp stem cells (Hamidouche et al. 2009; Fromigue et al. 2012; Cui et al. 2014). *itga5* knockdown using short hairpin RNAs in human dental pulp stem cells leads to a decrease in proliferation, and promotion of odontogenic differentiation (Cui et al. 2014). *Itga5* activity is mediated through FAK, PI3K, and ERK, which have a known role in proliferation, suggesting a potential mechanism, although proliferation was not directly assayed in this study (Hamidouche et al. 2009). *itga5* ultimately promotes an upregulation of osteoblast markers such as *runx2*, and increased osteogenesis (Hamidouche et al. 2009). In another study, Fromigue *et al.* show increased phospho-FAK and phosphorERK1/2 expression when *itga5* peptide is overexpressed coupled with a two- fold increase in bone thickness, yet they did not observe an increase in

Author Manuscript Author Manuscript Author Manuscript Author Manuscript

BrdU incorporation (Fromigue et al. 2012). Interestingly, previous data have shown that *itga5* mutants exhibit a hyoid arch defect, specifically a hypoplastic hyosymplectic (Crump et al. 2004) and variable posterior PA defects. We observe a more severe phenotype with the loss of both *prdm1a* and *itga5,* including loss of CB 2 which is derived from PA 3. Our data support a more posterior PA role for *itga5*, and this role is supported by experiments in the posterior cranial placode development (Bhat and Riley 2011). Furthermore, a role for *prdm1a* in the posterior cranial placodes has also been described, and localizes *itga5* and *prdm1a* to the same region (Bhat and Riley 2011; Culbertson et al. 2011). Though these studies do not directly assay for proliferation, *itga5* expression protects embryos from apoptosis as they observe a two-fold increase of apoptosis in *itga5* morphants (Bhat and Riley 2011). These data suggest that *itga5* acts via FGF8/MAP Kinase/PI3K signaling, and that this signaling pathway may be responsible for protecting against cell death (Bhat and Riley 2011). Since MAP Kinase family members do play a role in proliferation, it would be reasonable to hypothesize in the posterior pharyngeal arches, *prdm1a* through *itga5* promotes proliferation, possibly via MAP kinase family since our previous data show no change in apoptosis (Birkholz et al. 2009; Bhat and Riley 2011). Here we show that *itga5* expression is downregulated in *prdm1a* mutants, that *prdm1a* expression is also downregulated in *itga5* mutants, and that both *itga5* and *prdm1a* are both localized to the pharyngeal arches during craniofacial development. We further demonstrate that in double mutants, we observe a more severe phenotype and that the *prdm1a* mutant phenotype can be rescued with *itga5* mRNA. We further show that proliferation is decreased in *prdm1a* mutants and can be rescued with the addition of *itga5* mRNA. Taken together, our data show that there is an epistatic relationship between *prdm1a* and *itga5* where *itga5* expression can rescue the *prdm1a* mutant phenotype and a double mutant exhibits a more severe additive phenotype.

Methods

Zebrafish maintenance and lines

Zebrafish were cared for and maintained according to Westerfield's Zebrafish Book (Westerfield 1993). The TAB and AB wildtype strains were used (Zirc) and mutant lines include *prdm1a*^{m805} *(narrowminded(nrd))*(Artinger et al. 1999; Hernandez-Lagunas et al. 2005) and *itga5*^{b926} which were a generous gift from the Crump Lab (Crump et al. 2004); along with the tg[*prdm1a*::GFP] line (Elworthy et al. 2008). All embryos were staged following previously published standards for developmental staging (Kimmel et al. 1995) and mutants were genotyped using primers from the respective papers. All experiments utilizing zebrafish embryos conform to NIH regulatory standards of care and treatment and are approved by the UC Denver IACUC.

Morpholino and mRNA injections

Morpholino oligonucleotides (Gene Tools) were injected at the 1 cell stage with rhodamine-dextran (Sigma). *prdm1a* E2I2 splice site Morpholino was injected at 6 ng (Hernandez-Lagunas et al. 2005) and *itga5* exon-intron 13 splice site Morpholino (Crump et al. 2004) was also injected at 6 ng. *itga5* mRNA was amplified from 24 hpf cDNA isolated from whole embryos and cloned into pENTR/D-TOPO (Invitrogen) using the following primers:

Author Manuscript Author Manuscript Author Manuscript Author Manuscript

5′-GGTTAAGGACGTGAACCATCTCTTCG and 3′-GGGGATAGACACGTTCGTCCA. The *itga5* fragment was then put into pCS2+DEST using gateway cloning (Villefranc et al. 2007). *itga5* mRNA was synthesized using the mMessage mMachine kit (Ambion). mRNA was injected at the 1-cell stage at 50 pg, 90 pg, 112 pg and 136 pg. *prdm1a* and *itga5* mutant embryos were genotyped as described previously (Crump et al. 2004; Hernandez-Lagunas et al. 2005). Double mutant embryos were phenotyped for *prdm1a* mutant phenotypes, cut in half, and heads were used for staining and tails were genotyped.

In situ hybridization and Immunohistochemistry

Whole-mount RNA in situ hybridization (ISH) was performed as previously described (Thisse 1998) and visualized using the BM purple substrate (Roche). Fluorescent ISH was performed as previously described (Pineda et al. 2006; Powell et al. 2013). Briefly, a fluorescein conjugated antisense probe was synthesized from a full length pCS2+ GFP plasmid and used along with our antisense DIG conjugated probe for *itga5* (Zirc). Antisense DIG conjugated probes were synthesized from full-length sequences out of the pCS2+ plasmid for the following genes: *dlx2a* (Akimenko et al. 1994), *itga5* (ZIRC), *sox10* (Olesnicky et al. 2010), and *barx* (Sperber and Dawid 2008). Immunohistochemistry was performed as previously described (Ungos et al. 2003; Birkholz et al. 2009; Johnson et al. 2011) and the phosphohistone H3 antibody (Upstate) was used at 1:500 and the Alexa 568 Goat anti Rabbit (Invitrogen) at 1:750. Embryos were imaged on a Leica confocal for subsequent counting of phosphohistone H3 positive cells. We outlined the posterior arch domain and counted as previously described (Birkholz et al. 2009). A student's T-test was used to analyze significance between the groups.

Skeletal staining

Bone and cartilage staining was performed as previously described (Walker and Kimmel 2007; Johnson et al. 2011). Briefly, 5 dpf embryos were fixed for 1 hour at room temperature in 2% PFA, washed in 100 mM Tris pH 7.5/10 mM $MgCl_2$ buffer, then incubated overnight in 0.04% alcian blue (Anatech Ltd)/80% ETOH/10 mM $MgCl_2$. The next day, embryos were rehydrated through a series of ETOH washed and treated with 3% H2O2 to remove pigment then washed in 25% glycerol/0.1% KOH prior to alizarin red staining (0.5%, Sigma) for 30 minutes at room temperature and subsequent clearing and storage in 50% glycerol/0.1% KOH.

Supplementary Material

Refer to Web version on PubMed Central for supplementary material.

Acknowledgments

We thank past and present members of the Artinger lab especially Davalyn Powell, Morgan Singleton for excellent zebrafish care, Ana-Laura Hernandez for protocol troubleshooting, Leif Neitzel for dissection guidance, Adriana Estrada-Bernal for genotyping; Gage Crump for the *itga5* zebrafish line and reagents. This work is supported by NIDCR post-doctoral fellowship F32DE021920 to K.L, and NIH grant R01DE017699 to K.B.A., and P30NS048154 to the UC Denver zebrafish core facility.

Author Manuscript Author Manuscript Author Manuscript Author Manuscript

References

Akimenko MA, Ekker M, Wegner J, Lin W, Westerfield M. Combinatorial expression of three zebrafish genes related to distal-less: part of a homeobox gene code for the head. J Neurosci. 1994; 14:3475–3486. [PubMed: 7911517]

Artinger KB, Chitnis AB, Mercola M, Driever W. Zebrafish narrowminded suggests a genetic link between formation of neural crest and primary sensory neurons. Development. 1999; 126:3969–3979. [PubMed: 10457007]

Bachler M, Neubuser A. Expression of members of the Fgf family and their receptors during midfacial development. Mech Dev. 2001; 100:313–316. [PubMed: 11165488]

Bhat N, Riley BB. Integrin-alpha5 coordinates assembly of posterior cranial placodes in zebrafish and enhances Fgf-dependent regulation of otic/epibranchial cells. PLoS One. 2011; 6:e27778. [PubMed: 22164214]

Birkholz DA, Killian EC, George KM, Artinger KB. Prdm1a is necessary for posterior pharyngeal arch development in zebrafish. Dev Dyn. 2009; 238:2575–2587. [PubMed: 19777590]

Blentic A, Tandon P, Payton S, Walshe J, Carney T, Kelsh RN, Mason I, Graham A. The emergence of ectomesenchyme. Dev Dyn. 2008; 237:592–601. [PubMed: 18224711]

Chai Y, Maxson RE Jr. Recent advances in craniofacial morphogenesis. Dev Dyn. 2006; 235:2353–2375. [PubMed: 16680722]

Clouthier DE, Schilling TF. Understanding endothelin-1 function during craniofacial development in the mouse and zebrafish. Birth Defects Res C Embryo Today. 2004; 72:190–199. [PubMed: 15269892]

Clouthier DE, Williams SC, Yanagisawa H, Wieduwilt M, Richardson JA, Yanagisawa M. Signaling pathways crucial for craniofacial development revealed by endothelin-A receptor-deficient mice. Dev Biol. 2000; 217:10–24. [PubMed: 10625532]

Crump JG, Swartz ME, Kimmel CB. An integrin-dependent role of pouch endoderm in hyoid cartilage development. PLoS Biol. 2004; 2:E244. [PubMed: 15269787]

Cui L, Xu S, Ma D, Gao J, Liu Y, Yue J, Wu B. The role of integrin-alpha5 in the proliferation and odontogenic differentiation of human dental pulp stem cells. Journal of endodontics. 2014; 40:235–240. [PubMed: 24461410]

Culbertson MD, Lewis ZR, Nechiporuk AV. Chondrogenic and gliogenic subpopulations of neural crest play distinct roles during the assembly of epibranchial ganglia. PLoS One. 2011; 6:e24443. [PubMed: 21931719]

Eberhart JK, Swartz ME, Crump JG, Kimmel CB. Early Hedgehog signaling from neural to oral epithelium organizes anterior craniofacial development. Development. 2006; 133:1069–1077. [PubMed: 16481351]

Elworthy S, Hargrave M, Knight R, Mebus K, Ingham PW. Expression of multiple slow myosin heavy chain genes reveals a diversity of zebrafish slow twitch muscle fibres with differing requirements for Hedgehog and Prdm1 activity. Development. 2008; 135:2115–2126. [PubMed: 18480160]

Fromigue O, Brun J, Marty C, Da Nascimento S, Sonnet P, Marie PJ. Peptide-based activation of alpha5 integrin for promoting osteogenesis. Journal of cellular biochemistry. 2012; 113:3029–3038. [PubMed: 22566152]

Graham A. Development of the pharyngeal arches. American journal of medical genetics Part A. 2003; 119A:251–256. [PubMed: 12784288]

Hamidouche Z, Fromigue O, Ringe J, Haupl T, Vaudin P, Pages JC, Srouji S, Livne E, Marie PJ. Priming integrin alpha5 promotes human mesenchymal stromal cell osteoblast differentiation and osteogenesis. Proc Natl Acad Sci U S A. 2009; 106:18587–18591. [PubMed: 19843692]

Harburger DS, Calderwood DA. Integrin signalling at a glance. Journal of cell science. 2009; 122:159–163. [PubMed: 19118207]

Hernandez-Lagunas L, Choi IF, Kaji T, Simpson P, Hershey C, Zhou Y, Zon L, Mercola M, Artinger KB. Zebrafish narrowminded disrupts the transcription factor prdm1 and is required for neural crest and sensory neuron specification. Dev Biol. 2005; 278:347–357. [PubMed: 15680355]

Author Manuscript Author Manuscript Author Manuscript Author Manuscript

Johnson CW, Hernandez-Lagunas L, Feng W, Melvin VS, Williams T, Artinger KB. Vgll2a is required for neural crest cell survival during zebrafish craniofacial development. Dev Biol. 2011; 357:269–281. [PubMed: 21741961]

Julich D, Mould AP, Koper E, Holley SA. Control of extracellular matrix assembly along tissue boundaries via Integrin and Eph/Ephrin signaling. Development. 2009; 136:2913–2921. [PubMed: 19641014]

Kimmel CB, Ballard WW, Kimmel SR, Ullmann B, Schilling TF. Stages of embryonic development of the zebrafish. Dev Dyn. 1995; 203:253–310. [PubMed: 8589427]

Kopinke D, Sasine J, Swift J, Stephens WZ, Piotrowski T. Retinoic acid is required for endodermal pouch morphogenesis and not for pharyngeal endoderm specification. Dev Dyn. 2006; 235:2695–2709. [PubMed: 16871626]

Koshida S, Kishimoto Y, Ustumi H, Shimizu T, Furutani-Seiki M, Kondoh H, Takada S. Integrinalpha5-dependent fibronectin accumulation for maintenance of somite boundaries in zebrafish embryos. Dev Cell. 2005; 8:587–598. [PubMed: 15809040]

Le Douarin, NM. The neural crest. Cambridge Univ Press; New York: 1982.

Nechiporuk A, Linbo T, Poss KD, Raible DW. Specification of epibranchial placodes in zebrafish. Development. 2007; 134:611–623. [PubMed: 17215310]

Olesnicky E, Hernandez-Lagunas L, Artinger KB. prdm1a Regulates sox10 and islet1 in the development of neural crest and Rohon-Beard sensory neurons. Genesis. 2010; 48:656–666. [PubMed: 20836130]

Pineda RH, Svoboda KR, Wright MA, Taylor AD, Novak AE, Gamse JT, Eisen JS, Ribera AB. Knockdown of Nav1.6a Na+ channels affects zebrafish motoneuron development. Development. 2006; 133:3827–3836. [PubMed: 16943272]

Powell DR, Hernandez-Lagunas L, LaMonica K, Artinger KB. Prdm1a directly activates foxd3 and tfap2a during zebrafish neural crest specification. Development. 2013; 140:3445–3455. [PubMed: 23900542]

Schilling TF, Kimmel CB. Segment and cell type lineage restrictions during pharyngeal arch development in the zebrafish embryo. Development. 1994; 120:483–494. [PubMed: 8162849]

Sperber SM, Dawid IB. barx1 is necessary for ectomesenchyme proliferation and osteochondroprogenitor condensation in the zebrafish pharyngeal arches. Dev Biol. 2008; 321:101–110. [PubMed: 18590717]

Thisse, CaTB. High resolution whole-mount in situ hybridization. Zebrafish Science Monitor. 1998; 15:8–9.

Ungos JM, Karlstrom RO, Raible DW. Hedgehog signaling is directly required for the development of zebrafish dorsal root ganglia neurons. Development. 2003; 130:5351–5362. [PubMed: 13129844]

Villefranc JA, Amigo J, Lawson ND. Gateway compatible vectors for analysis of gene function in the zebrafish. Dev Dyn. 2007; 236:3077–3087. [PubMed: 17948311]

Walker MB, Kimmel CB. A two-color acid-free cartilage and bone stain for zebrafish larvae. Biotechnic & histochemistry: official publication of the Biological Stain Commission. 2007; 82:23–28. [PubMed: 17510811]

Westerfield, M. The Zebrafish Book: A guide for the laboratory use of zebrafish (Danio rerio). University of Oregon Press; Eugene: 1993.

Wilm TP, Solnica-Krezel L. Essential roles of a zebrafish prdm1/blimp1 homolog in embryo patterning and organogenesis. Development. 2005; 132:393–404. [PubMed: 15623803]

Yang JT, Rayburn H, Hynes RO. Embryonic mesodermal defects in alpha 5 integrin-deficient mice. Development. 1993; 119:1093–1105. [PubMed: 7508365]

Author Manuscript Author Manuscript Author Manuscript Author Manuscript

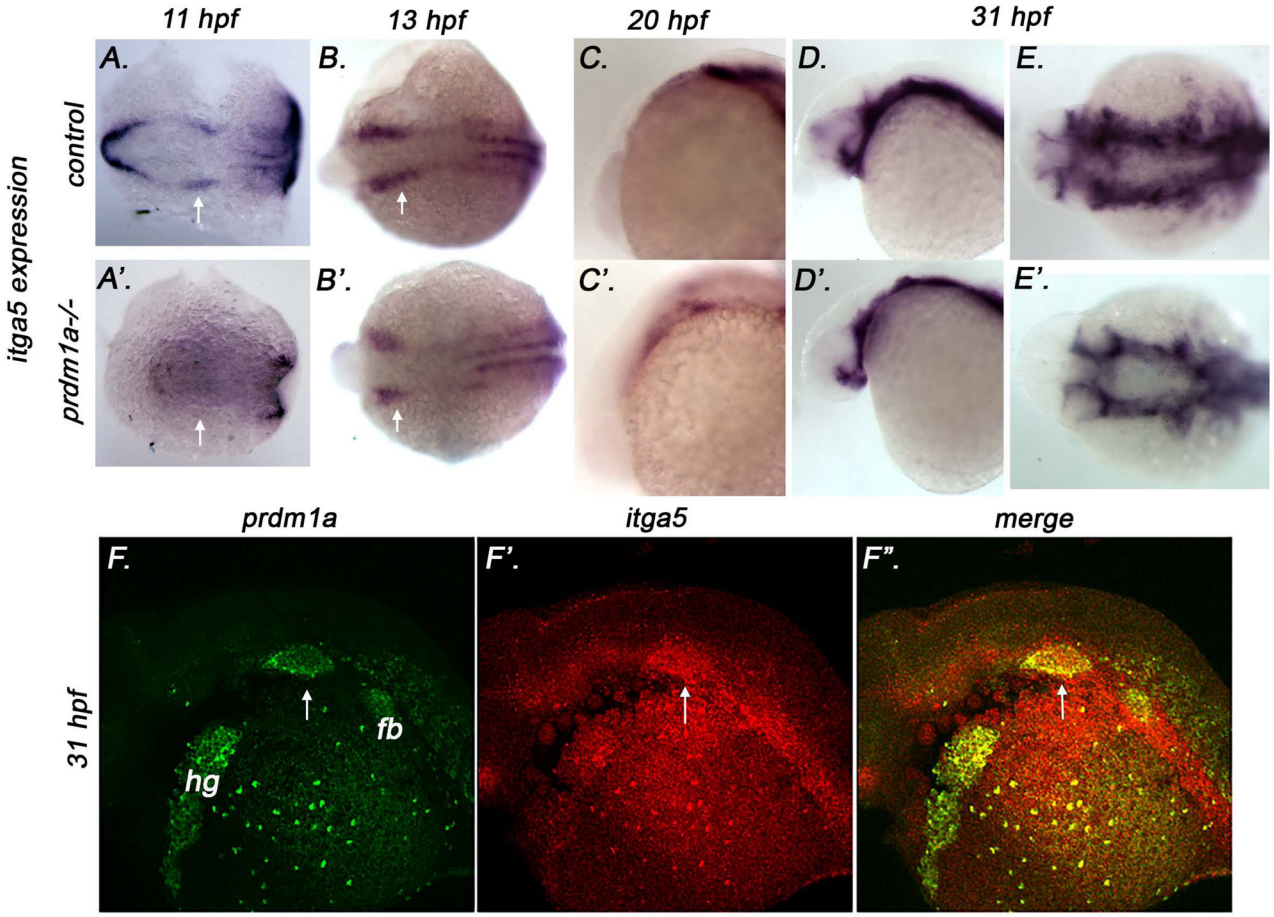

Figure 1. *itga5* is expressed in the posterior pharyngeal arch domain and is reduced in *prdm1a* mutants

itga5 mRNA expression by ISH in wild type and *prdm1a* mutant embryos. Lateral views, anterior is to the left. Wildtype expression of *itga5* at 11 hpf (A), 13 hpf (B), 20 hpf (C.), and 31 hpf (D (lateral), E (dorsal). *prdm1a* mutant embryos have reduced expression of *itga5* in the pharyngeal arches (arrows) at 11 hpf (A′), 13 hpf (B′.), 20 hpf (C′), and 31 hpf (D′ (lateral), E′ (dorsal) as observed in 25% of embryos that are homozygous mutant expected from a heterozygous cross. (F, F′F″) Confocal projected image of double Fluorescent ISH for *itga5* and *prdm1a* representing a compressed stack at 10x magnification. Anterior is to the left. At 31 hpf *prdm1a:gfp* is expressed in the posterior PAs, hatching gland (hg), fin bud (fb) (F). *itga5* is expressed in the PAs (F′). Both *itga5* and *prdm1a* localize to the posterior PAs (yellow in F″). The apparent expression of *itga5* that is punctate in the area of the hatching gland we consider to be background staining.

Author Manuscript Author Manuscript Author Manuscript Author Manuscript

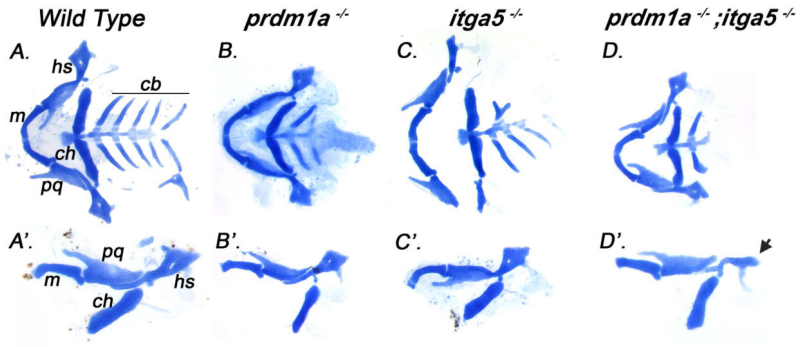

Figure 2. Double mutants for *itga5* and *prdm1a* results in an additive viscerocranium phenotype

Ventral (A–D) and lateral (A′–D′) views, anterior is to the left. Paired images are from two different embryos. Flat mounts of alcian blue staining for cartilaginous elements at 5 dpf shows *itga5* and *prdm1a* double mutants results in an additive effect. All phenotypes were confirmed by genotyping. (A, A′) Wild type embryos show the normal pattern of the viserocranium. *prdm1a* mutants are lacking cbs 3-5 (n=16; B, B′) and in *itga5* mutants, a fusion between cbs 1-2 is observed followed by a loss of posterior ceratobranchials on the same side (C, C′) while the other side is lacking cb 5 (n=4 only confirmed by genotyping since we selected for *prdm1a* mutant phenotypes before genotyping). In some embryos, the foramen of the hyosymplectic is reduced (see arrow in D′). The double *prdm1a*$^{-/-}$*itga5*$^{-/-}$ mutants are lacking all posterior CBs except CB1 (D, D′) and a reduced hyosymplectic (n=15 confirmed by genotyping from 4 different clutches). m-meckels, pq-palatoquadrate, hs-hyosymplectic, ch-ceratohyal, cb-ceratobranchials.

Author Manuscript Author Manuscript Author Manuscript Author Manuscript

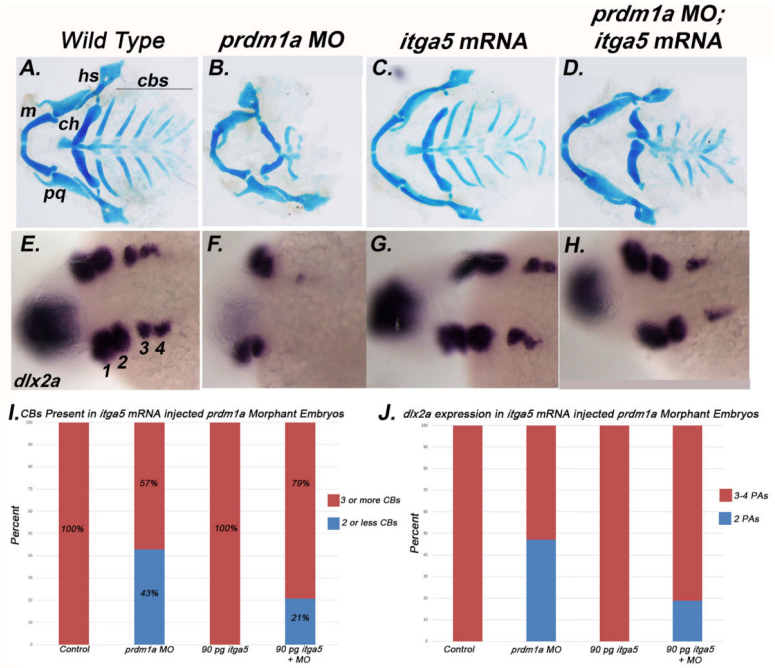

Figure 3. Overexpression of *itga5* mRNA in *prdm1a* morphants results in rescue of the ceratobrancial cartilages in *prdm1a* mutants

Anterior is to the left. (A–D) Ventral views of alcian staining for cartilaginous elements at 6 dpf showing that *prdm1a* morphants injected with *itga5* mRNA rescues cbs (D, I) compared to *prdm1a* morphants (B, I), wild type, and *itga5* mRNA (C, I). (n= WT=86/86, 3 or more cbs, *prdm1a*-MO= 6/14, 2 or less cbs (as shown in B) and 8/16, 3 or more cbs, itga5a mRNA= 49/49, 3 or more cbs (as shown in C), and *prdm1a*-MO rescued with *itga5* mRNA =12/58, 2 or less cbs and 46/58, 3 or more cbs (as shown in D). *dlx2a* expression is rescued at 24 hpf with injection of *itga5a* mRNA in *prdm1a* morphants (H, J) to a level similar to wild type (E, J) (n= WT=18/18, 3 or more cbs (as shown in E), *prdm1a*-MO= 9/17, 3 or more cbs and 8/17, 2 or less cbs (as shown in F), itga5a mRNA= 7/7, 3 or more cbs (as shown in G), *prdm1a*-MO rescued with *itga5* mRNA =13/16 (as shown in H). Quantification of the number of CBs and PAs in all conditions is shown in (F, J) from 3 different clutches. m-meckels, p-palatoquadrate, hs-hyosymplectic, ch-ceratohyal, cb-ceratobranchials.

Author Manuscript Author Manuscript Author Manuscript Author Manuscript

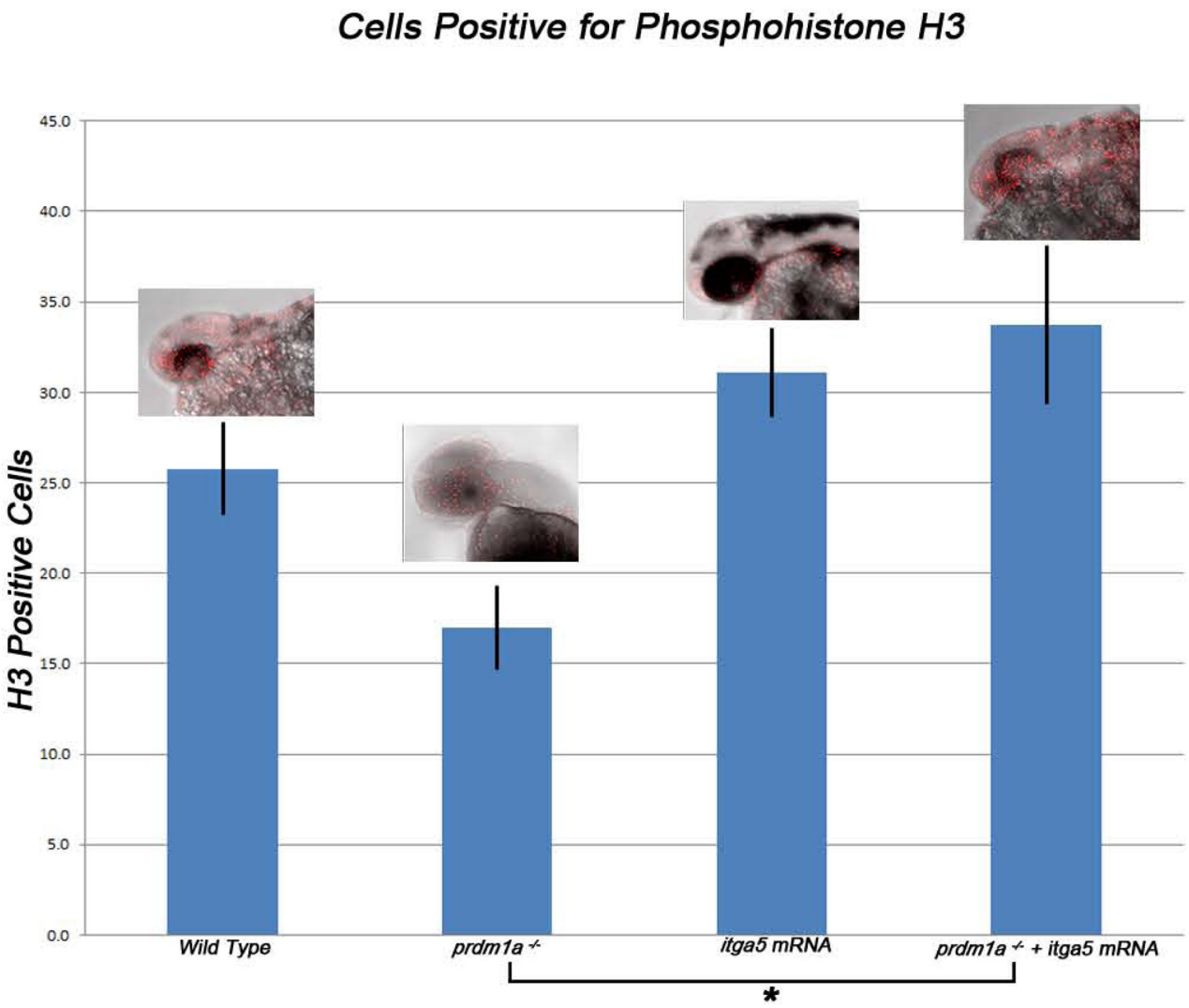

Figure 4. Overexpression of *itga5* mRNA in *prdm1a* mutants recues cellular proliferation

Quantification of the number of phosphohistone H3 positive cells in all conditions, insets show representative images of whole mount embryos labeled with red phosphohistone H3 positive cells. Wild type embryos contain an average of 25 positive cells in the PA region similar to i*tga5* mRNA injected alone, while *prdm1a* mutants have significantly less cell proliferation with an average of 17 positive cells. *prdm1a* mutants injected with *itga5* mRNA have a significantly higher rate of proliferation than what is observed in *prdm1a* mutants alone ($p<0.05$ by Student's T-test, comparing mutant to *prdm1a* mutants injected with *itga5* mRNA (as shown by the asterix on the figure); n= WT=9, *prdm1a*-mutant=8, itga5a mRNA=4, rescue=9). There is no significant difference between *itga5* mRNA and wild type, rescue and wild type, and itga5 mRNA and rescue ($p>0.05$), showing the rescue is similar to the wild type and mRNA alone.